Location- and Orientation-Aided Millimeter Wave Beam Selection Using Deep Learning

Rezaie, Sajad; Manchon, Carles Navarro; De Carvalho, Elisabeth

Published in:
ICC 2020 - 2020 IEEE International Conference on Communications (ICC)

DOI (link to publication from Publisher):
10.1109/ICC40277.2020.9149272

Publication date:
2020

Document Version
Accepted author manuscript, peer reviewed version

Location- and Orientation-Aided Millimeter Wave Beam Selection Using Deep Learning

Sajad Rezaie, Carles Navarro Manchón, Elisabeth de Carvalho
Department of Electronic Systems, Aalborg University, Denmark
Email: {sre, cnm, edc}@es.aau.dk

***Abstract*—Location-aided beam alignment methods exploit the user location and prior knowledge of the propagation environment to identify the beam directions that are more likely to maximize the beamforming gain, allowing for a reduction of the beam training overhead. They have been especially popular for vehicle to everything (V2X) applications where the receive array orientation is approximately constant for each considered location, but are not directly applicable to pedestrian applications with arbitrary orientation of the user handset. This paper proposes a deep neural network based beam selection method that leverages position and orientation of the receiver to recommend a shortlist of the best beam pairs, thus significantly reducing the alignment overhead. Moreover, we use multi-labeled classification to not only capture the beam pair with highest received strength but also enrich the neural network with information of alternative beam pairs with high received signal strength, providing robustness against blockage. Simulation results show the better performance of the proposed method compared to a generalization of the inverse fingerprinting algorithm in terms of the misalignment and outage probabilities.**

I. Introduction

Beyond 5G systems will serve the recent emerging services, such as high-definition multimedia applications as well as virtual and augmented reality, where ultra high throughput is required. Such high throughput can be obtained by accessing the millimeter wave (mmWave) band, which offers enormous and continuous unallocated bandwidth [1]–[3]. MmWave communication can moreover be easily used in small cells due to higher propagation and penetration loss at mmWave frequencies; nonetheless, high penetration losses cause common blockage, which makes it difficult to establish a reliable mmWave link. Directional beamforming using multiple-input multiple-output (MIMO) antenna arrays with large number of elements is frequently employed to obtain a sufficient link budget, thanks to the array gain. To do this successfully, transmitter and receiver need to align their transmissions over the direction of the line-of-sight (LOS) channel component, or a strong non-line-of-sight (NLOS) path when the LOS is blocked. As a result, configuring antenna arrays at transmitter and/or receiver is challenging in highly dynamic propagation environments [2].

Commonly, codebook-based analog beamforming with a set of predefined beams has been proposed to reduce the complexity of the arrays configuration and alignment process. Typically, the set of predefined beams in the codebook is realized via analog beamforming or a combination of digital and analog processing. Although an exhaustive search procedure over all beam pairs in the codebooks yields the optimal beam pairs in high signal-to-noise ratio (SNR) conditions, it requires unacceptably high latency and overhead. On the other hand, hierarchical search algorithms have lower overhead but there is no guarantee to cover cell edges [4]. Context information (CI)-based beam alignment methods were proposed to leverage contextual information such as user location to overcome these challenges. The authors of [3] proposed a data-driven beam alignment method for mmWave vehicle to infrastructure (V2I) communication which utilizes multipath fingerprints and position information to extend CI-based beam alignment in the case of NLOS links. To reduce effects of imperfect position information at both ends, one approach based on Bayesian decision theory has been proposed in [5]. In [10], the authors propose a beam selection scheme that, in addition, estimates the position and orientation of receiver in each step of beam alignment procedure, showing that the position/orientation estimation and the beam alignment procedures benefit from each other.

As another strategy, machine learning based beam alignment methods have been proposed to use the high capacity of kernel based models and neural networks (NN) in learning the non-linearities present in the function mapping the best beam pair with highest received power and receiver location [6], [7]. Due to the opportunity of using additional information in vehicular scenarios, RADAR and LIDAR based beam alignments were proposed to capture more information about obstacles in environment [8], [9]. However, the mentioned machine learning methods deal with V2X applications in which the receiver array orientation can be directly inferred from the vehicle position. As such, they cannot be applied to indoor scenarios with pedestrian users where receivers can take any arbitrary orientation. Note that directional beam codebooks are typically made of beams with different beamwidths and, therefore, the transformation that a receiver rotation imposes on the received signal strength of each possible beam pair cannot be deterministically predicted, even when the rotation angle is perfectly known.

In this paper, we propose a new data-driven beam selection method for mmWave communications that leverages both orientation and location information of users. We consider an indoor scenario in which, contrary to the vehicular ap-

This work is supported by the Danish Council for Independent Research, grant no. DFF 8022-00371B.

plications, the receivers can take any arbitrary orientation and position. In addition, the environment includes static and mobile scattering objects, which reflect and block the multipath components complicating the beam selection task. Since deep learning is able to capture the structure of the environment, we propose a deep neural network structure for classification that takes as input the position and orientation of the receiver, and outputs probabilities of being the best for each beam-pair. The overhead of beam selection procedure is reduced significantly by sensing only beam pairs with high probabilities.

As another contribution, we apply multi-label classification to enhance the procedure of learning the environment's structure by training the model in the direction of not only the most powerful path but also alternative paths with high power. This endows the proposed model with robustness against mismatches in the training data. Furthermore, in order to compare the proposed method with a data driven based algorithm, we generalize the inverse fingerprinting method proposed by [3] to work with varying receiver orientation. Our numerical results show that the proposed framework offers a performance close to that of perfect beam alignment and significantly superior to that of the generalized inverse fingerprinting (GIFP) method trained with identical data.

II. System Model

We consider a 2D indoor downlink scenario where one transmitter and one receiver with N_t and N_r antennas, respectively, want to establish a mmWave communication link.

A. Channel Model

Due to the importance of location information for fast beam alignment in mmWave communication, we use a 2-dimensional (2D) geometric based channel model proposed by [11]. In this model, objects in the environment such as building, equipment, and humans are mapped to 2D rectangular or circular objects. In each realization, we define mobile scatterers with varying position and orientation, in contrast to static scatterers with fixed position and orientation, to simulate mobile blockers. For simplicity, we place the transmitter at position $\boldsymbol{p}_t = (0, 0)$ with fixed angle of its antenna array α_t, with respect to the x-axis. As depicted in Fig. 1, the receiver can take any position $\boldsymbol{p}_r = (x_r, y_r) \in \mathbb{R}^2$ with random orientation $\alpha_r \in [0, 2\pi)$ where there is no overlap with other static or mobile objects.

In addition to the LOS path between transmitter and receiver, we consider first, second, and third order reflection of static and/or mobile rectangular objects using image theory [11], [12]. We apply a narrowband channel model to the contribution of one LOS and L NLOS paths,

$$\boldsymbol{H} = \sum_{l=0}^{L} \sqrt{N_t N_r}\, \beta_l\, c_l\, \boldsymbol{a}_r(\theta_{r,l})\, \boldsymbol{a}_t^H(\theta_{t,l}), \tag{1}$$

in which $\boldsymbol{H}$ and $c_l \in [0, 1]$ denotes the $N_R \times N_T$ channel matrix and transfer coefficient of lth path due to penetration loss by blockers[1], respectively. $\beta_l \in \mathcal{CN}(0, \sigma_l^2)$ is the complex fading gain of lth path with variance $\sigma_l^2 \propto d_l^{-\gamma}$, where d_l and γ are the distance that lth path traverses to the receiver and path loss exponent, respectively. Also, $\theta_{r,l}$, $\theta_{t,l}$, $\boldsymbol{a}_r(\theta_{r,l})$ and $\boldsymbol{a}_t(\theta_{t,l})$ are the angle of arrival (AoA) and angle of departure (AoD) with respect of the array axis, the antenna array response of receiver and transmitter, respectively. We consider uniform linear arrays (ULA) of ideal isotropic antenna elements with $\lambda/2$ antenna spacing, yielding the array responses

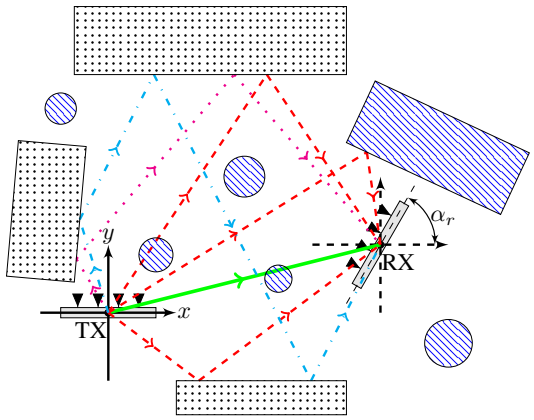

Fig. 1. 2D mmWave system model including a fixed TX, a mobile RX, 3 static objects (black), and 6 mobile objects (blue) for a given realization with one LOS path and $L = 5$ reflected paths.

$$\boldsymbol{a}_r(\theta_{r,l}) = \frac{1}{\sqrt{N_r}}[1, e^{-j\pi cos(\theta_{r,l})}, \ldots, e^{-j\pi(N_r-1)cos(\theta_{r,l})}]^T, \tag{2}$$

$$\boldsymbol{a}_t(\theta_{t,l}) = \frac{1}{\sqrt{N_t}}[1, e^{-j\pi cos(\theta_{t,l})}, \ldots, e^{-j\pi(N_t-1)cos(\theta_{t,l})}]^T. \tag{3}$$

B. Beam Codebook

In analog beamforming, the beamforming operations are performed in the analog domain by connecting each antenna to one analog phase shifter. We assume a codebook-based analog beamforming architecture to beamform signals with a single RF chain at transmitter and receiver. We denote by $\mathcal{F} = \{\boldsymbol{f}_1, \ldots, \boldsymbol{f}_{N_t}\}$ and $\mathcal{W} = \{\boldsymbol{w}_1, \ldots, \boldsymbol{w}_{N_r}\}$ the codebooks used for analog beamforming at the transmitter and analog combining at the receiver, each of them with N_t and N_r beams, respectively. We use the common Discrete Fourier transform (DFT)-based codebooks [5], [13] with precoders and combiners reading

$$\boldsymbol{f}_p = \frac{1}{\sqrt{N_t}}[1, e^{-j\pi \frac{2p-1-N_t}{N_t}}, \ldots, e^{-j\pi(N_t-1)\frac{2p-1-N_t}{N_t}}]^T, \tag{4}$$

$$\boldsymbol{w}_q = \frac{1}{\sqrt{N_r}}[1, e^{-j\pi \frac{2q-1-N_r}{N_r}}, \ldots, e^{-j\pi(N_r-1)\frac{2q-1-N_r}{N_r}}]^T, \tag{5}$$

[1]To consider effects of blockers on lth path, we consider a simple model as $c_l = \eta^{n_l}$, where η and n_l denote the transmission coefficient of objects and the number of objects which have intersection with the lth path, respectively.

where $p \in \{1, \ldots, N_t\}$ and $q \in \{1, \ldots, N_r\}$.

On each time slot, according to the precoder $\boldsymbol{f}_p \in \mathcal{F}$ and combiner $\boldsymbol{w}_q \in \mathcal{W}$, the received signal power $\mathbf{R} \in \mathbb{R}^{N_t \times N_r}$ can be written as

$$\mathbf{R}[p,q] = \left\| \sqrt{P_t} \boldsymbol{w}_q^H \boldsymbol{H} \boldsymbol{f}_p s + \boldsymbol{w}_q^H \boldsymbol{n} \right\|^2 \quad (6)$$

in which P_t, $s \in \mathbb{C}$, and $\boldsymbol{n} \in \mathbb{C}^{N_r}$ denote the transmission power, the known training symbol with normalized power, and a zero mean complex Gaussian noise vector with variance σ_n^2.

III. Data-Driven Beam Selection

Besides prior knowledge of the propagation environment, position and orientation of RX ($\boldsymbol{p}_r$ and α_r) can be used to reduce the overhead of the beam alignment procedure. The prior knowledge of the environment is acquired from measurements in a training phase, which are collected in the target environment. Each sample of the training data corresponds to a realization of the environment where the receiver and mobile objects take an arbitrary location and orientation. The training data includes position and orientation of receiver in addition to the measured received signal strength for all combinations of $\mathcal{F}$ and $\mathcal{W}$. Thus for a given realization of the environment, according to the prior knowledge and the location and orientation of the receiver, data-driven methods recommend a shortlist of beam pairs to limit the search space of finding the best beam pair with the highest received strength.

As mentioned in Section I, probabilistic and machine learning based beam selections are two common types of data-driven procedures to exploit the prior information of the environment for a given receiver location. To give a comparison between these two approaches, we use the inverse fingerprinting (IFP) beam selection method [3] as a baseline of comparison with the proposed machine learning based approach. However, the IFP method considers only the location of vehicles, not taking into account the arbitrary orientation of the receiver array. Moreover, knowledge of the beam direction recommended by the IFP method at angle α_{r_1} does not determine the corresponding unique beam direction at angle α_{r_2}, due to the beam patterns having unequal beamwidths in the DFT-based codebook. Therefore, we extend the IFP method to be able to select beam pairs in varying receiver angles.

A. Generalized Inverse fingerprinting Method

To consider the orientation of receivers in the IFP method, bin definition is extended to discretize both the spatial and angular domains. As depicted in Fig. 2, the corresponding bin of each observation is determined using position and angle of the receiver ($\boldsymbol{p}_r$ and α_r). The kth bin is defined as:

$$\mathcal{B}_k = [x_k, x_k + \Delta_s) \times [y_k, y_k + \Delta_s) \times [\alpha_k, \alpha_k + \Delta_a), \quad (7)$$

where Δ_s and Δ_a denotes spatial bin size (SBS) and angular bin size (ABS), respectively. Also, by setting $\Delta_a = 2\pi$ we recover the classical IFP bin definition.

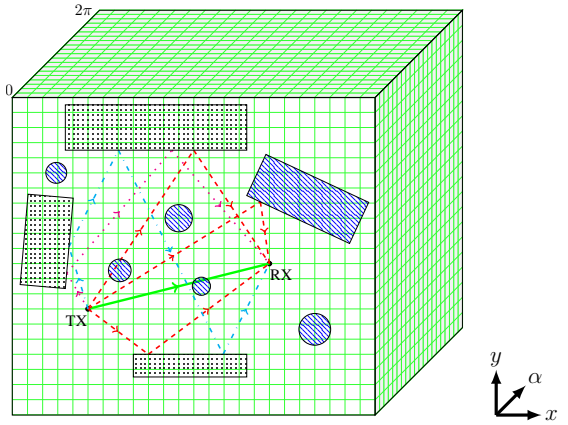

Fig. 2. Bin definition in Generalized Inverse Fingerprinting beam alignment. The third dimension is used only to show impacts of orientation in bin definition procedure.

Similar to the IFP method, a set of N_b candidate beam pairs of the kth bin, denoted by $\mathcal{S}_k$, is selected to minimize the probability of not containing the beam pair with the highest received power in it. We define this probability as the misalignment probability, and it can be expressed as

$$P_m(\mathcal{S}_k) = \mathbb{P}\left[\max_{(i,j) \in \mathcal{S}_k} \mathbf{R}[i,j] < \max_{(p,q) \in \mathcal{B}} \mathbf{R}[p,q] \right], \quad (8)$$

where $\mathcal{B}$ denotes the set of all possible beam pair combinations. In [3], it is proved that $\mathcal{S}_k$ is equivalent to the top N_b ranked beam pairs according to their frequency of being best in the training observations associated with the kth bin. Due to the increased number of bins in GIFP compared to conventional IFP, more training data is needed to reach the same number of training samples per bin.

B. Proposed Deep-Learning Based Method

The presence in the environment of static and mobile scatterers, which can block or reflect the multipath components with highest power, implies that beam selection using context information is a highly nonlinear classification problem. While support vector machine (SVM) and shallow neural networks have the ability to classify linear and slightly nonlinear problems by hyperplane separators, a deep neural network is able to learn highly complex nonlinear functions by adding hidden layers. We hence select a deep neural network model for classification as explained in the following.

As depicted in Fig. 3, we consider a deep neural network with 3 inputs, corresponding to the receiver's location (x_r, y_r) and its orientation α_r. The network is made 5 fully-connected hidden layers so that it has enough depth to learn the non-linearities present in a highly crowded environment. To enable the capacity of the neural network to learn non-linearities, we use tanh and Softmax functions as the activation functions in the hidden layers and the output layer, respectively. Each of the hidden layers contains N_{hid} neurons, while the output layer is made of $N_t N_r$ outputs, one for each possible beam pair. This results in a total of $4N_{\text{hid}} + 4N_{\text{hid}}(N_{\text{hid}}+1) + (N_{\text{hid}}+1)N_t N_r$ trainable parameters.

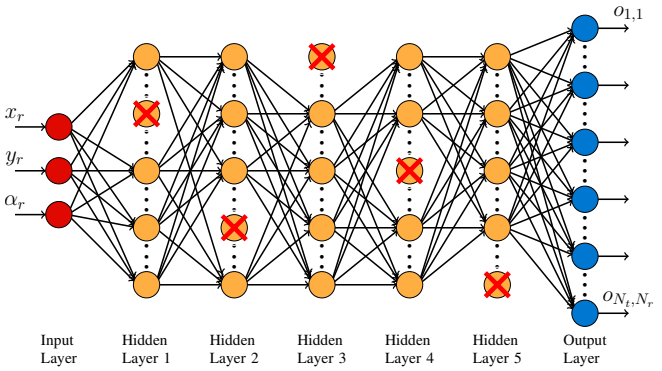

Fig. 3. Deep neural network architecture of the proposed beam alignment method using context information.

We configure the neural network to learn the index of the best beam pair by labeling the outputs $\mathcal{O} = \{o_{i,j} | i = 1, \ldots, N_t; j = 1, \ldots, N_r\}$ of the training data as

$$o_{i,j} = \begin{cases} 1, & \text{if } (i,j) = \arg\max_{m,n} \mathbf{R}[m,n], \\ 0, & \text{otherwise.} \end{cases} \tag{9}$$

This implies that $\mathcal{O}$ has only one nonzero member $o_{m,n}$, where m and n are the indices of TX and RX beam of the best beam pair, respectively.

Overfitting occurs when a neural network is trained on a small or not large enough dataset and degrades the performance of the neural network on test data. To overcome this problem, we use dropout as a regularization mechanism. Dropout attempts to combine different structures of neural networks to prevent memorizing the training data [14]. In this technique, as depicted in Fig. 3, some nodes of a specific layer are dropped out randomly in each batch of training data. We set a dropout ratio $p = 0.1$ to give up 10% of nodes in each hidden layer randomly. The dropped out nodes are illustrated by red cross marks in Fig. 3.

In test mode, the inputs of the neural network are fed with the position and angle of the receiver. Since the activation function of the output layer is Softmax, the neural network generates the probability of being best for all beam pairs. The candidate list of beam pairs can be chosen by truncating the N_b first indices of the outputs sorted in descending order, i.e.,

$$\begin{aligned} \boldsymbol{g} &= \arg\operatorname*{sort}_{i,j} (o_{i,j}), \\ \mathcal{S} &= \{\boldsymbol{g}(k) | k = 1, \ldots, N_b\}. \end{aligned} \tag{10}$$

Multi-label classification: Both inverse fingerprinting and single-labeled classifier beam alignment methods focus on the path with highest power and, consequently, these methods need large training datasets to yield acceptable accuracy especially in highly crowded scenarios. To overcome this problem, we propose to use multi-label classification to capture not only the best beam pair but also the remaining high power beam pairs in the training data. By adding this data to our training labels, the neural network can learn other paths between transmitter and receiver. The output label during the training phase of the M-labeled classification should be revised as:

$$\begin{aligned} \boldsymbol{r} &= \arg\operatorname*{sort}_{i,j} (\mathbf{R}[i,j]), \\ \mathcal{T} &= \{\boldsymbol{r}(k) | k = 1, \ldots, M\}, \\ o_{i,j} &= \begin{cases} 1, & \text{if } (i,j) \in \mathcal{T}, \\ 0, & \text{otherwise,} \end{cases} \end{aligned} \tag{11}$$

where the kth element of $\boldsymbol{r}$ contains the indices of the kth highest value in $\mathbf{R}$, and $\mathcal{T}$ contains the first M elements of $\boldsymbol{r}$. Thus, M outputs are labelled with a 1 in $\mathcal{O}$, which correspond to the top-M beam pairs with the highest received power.

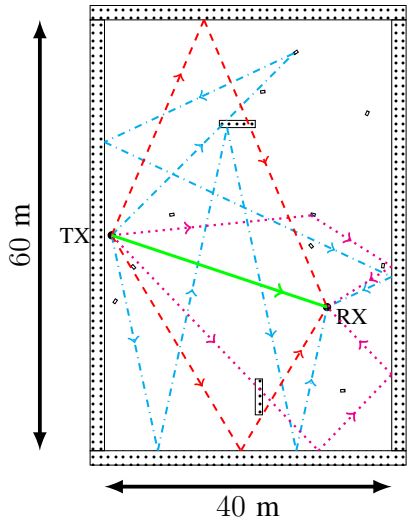

Fig. 4. An Indoor mmWave system model with 6 static and 10 mobile objects. In addition to LOS, to have better representation, only 6 NLOS paths are drawn among all 24 reflected paths.

IV. Simulation Results and Discussions

This section presents simulation results of the proposed deep learning based beam alignment method and compares it with the generalized inverse fingerprinting as the baseline method. To make a fair comparison between these methods, we calculate performance metrics by feeding both of them with same training and test data. We consider 6 static objects, including four walls and two fixed obstacles, in addition to varying the number of mobile objects to model an indoor environment. The parameters used for channel modeling are $N_t = 64$, $N_r = 64$, $\gamma = 2$, $P_t = 24$ dBm, and $\sigma_n^2 = -84$ dBm. Also, the reflection coefficient and the transmission coefficient of all objects are $\Gamma = 0.4$ and $\eta = 0.05$, respectively. Fig. 4 depicts the indoor scenario where a transmitter, which is placed at a distance of 1 m from the left wall, communicates with a receiver placed randomly in the room. Code to replicate the results can be found in https://github.com/SajadRezaie/OriLocBeamSelection.

A. Generation of Training and Test Datasets

In each realization of the environment, mobile objects are newly drawn inside of the room according to a two-dimensional homogeneous Poisson point process with mean

number of points λ, while static objects preserve always the same position and orientation over all environment realizations. The mobile objects' size is chosen in order to model the effect of pedestrians with dimension $0.35\text{m} \times 0.6\text{m}$. A receiver is placed randomly inside of the room where there is no overlap with the static and mobile objects. In this scenario, some or all paths may be blocked due to the two fixed obstacles inside the room with dimension $5\text{m} \times 1\text{m}$ and other mobile objects.

Based on image theory, the probability of having a reflected path reaching the receiver from a given object is proportional to the object's dimensions. Moreover, higher order reflected paths reach the receiver after more than one reflection with the objects [11]. Since, in the considered indoor scenario, mobile objects are much smaller than static ones, the probability of a having a reflected path from more than one mobile objects reaching the receiver is close to zero, in addition to those paths having much smaller signal energy than lower-order ones. Therefore, we disregard paths with reflections from more than one mobile objects to reduce the computation time of the ray tracing procedure. The received signal power in each beam pair is saved in a dataset, which we randomly split into two groups: 80% of data is dedicated for training and the remaining part for evaluating performance of the beam alignment methods.

B. Numerical Evaluation

According to the $N_t N_r = 4096$ neurons in the last layer of neural network and using $N_{\text{hid}} = 128$ neurons in each hidden layer, there are 594944 trainable weights in the network. Since the number of neurons in the output layer is 32 times larger than N_{hid}, more than 88% of the trainable weights are located in the last dense layer. We use Adam optimizer and train the deep neural network with 50 epochs with minibatch size progressively increasing from 32 to 8192 examples. Fig. 5 shows the misalignment probability of the proposed method, according to (8), in comparison with the GIFP method with different spatial and angular bin sizes by processing two datasets A and B with $10,000$ and $100,000$ samples, respectively. The performance of GIFP method is very dependent to the values of SBS and ABS. Basically, there is a tradeoff on the selection of the bin sizes, whose optimal setting depends on the dataset size. On the one hand, larger bin sizes allow more data samples per bin, which results in obtaining better statistics for construction of the list of beam candidates. On the other hand, though, larger bins result in lower spatial resolution and the bundling together of positions for which the optimal beam pairs are significantly different. Anyway, the deep learning based method always outperforms the GIFP method with various values of SBS and ABS. Using multi-label classification decreases the misalignment probability of the proposed method with respect to the single-labeled one. Since the multi-labeling technique can be seen as a data augmentation strategy, it has a stronger impact on the results of dataset A which includes fewer samples.

To evaluate the robustness of the multi-labeled deep learning based beam alignment in indoor mmWave communications,

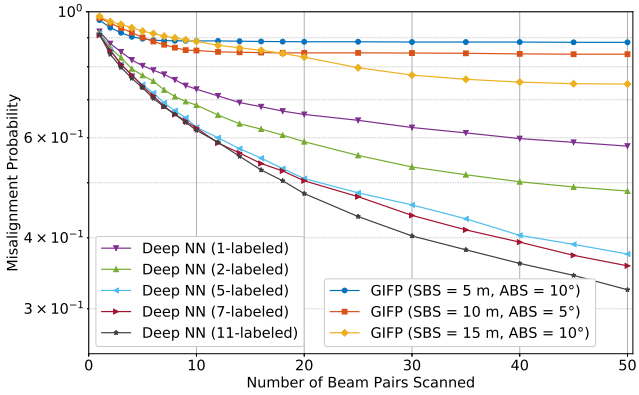

(a) Dataset A with $10,000$ samples

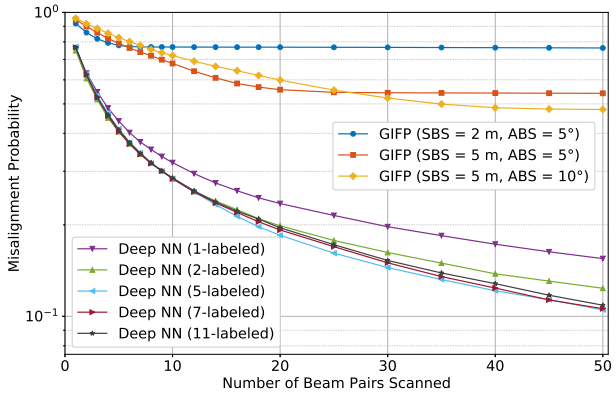

(b) Dataset B with $100,000$ samples

Fig. 5. Misalignment probability of deep learning based beam alignment and GIFP method with different spatial and angular bin sizes when $\lambda = 10$.

we use the outage probability and achievable spectral efficiency in the same scenario. The outage probability of a link is defined as the probability that the signal to noise ratio (SNR) corresponding to a given pair of the precoder and combiner is smaller than a required threshold level SNR_{TH}. The SNR corresponding to the beam pair (p, q) is defined as

$$\text{SNR}_{p,q} = \frac{\left\| \sqrt{P_t} \boldsymbol{w}_q^H \boldsymbol{H} \boldsymbol{f}_p \boldsymbol{s} \right\|^2}{\sigma_n^2}. \tag{12}$$

In the following simulation, we set $\text{SNR}_{\text{TH}} = 20\text{dB}$. In addition, the achievable spectral efficiency of beam pair (p, q) can be calculated as

$$\text{SE}_{p,q} = \log_2(1 + \text{SNR}_{p,q}). \tag{13}$$

As Fig. 6 demonstrates, deep neural network based beam selection has lower outage probability than GIFP method with the same number of recommended beam pairs. Moreover, by increasing the number of labels at the multi-label classification, the loss of the deep learning method with respect to the perfect beam alignment is reduced.

A usual concern when using data-based approaches is the robustness of a model trained in a certain environment when evaluated in an environment with mismatched characteristics. In vehicular to infrastructure mmWave networks performance

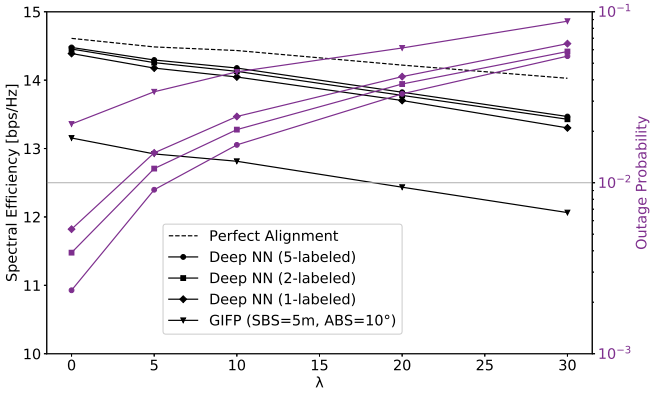

Fig. 6. Spectral efficiency (black) and outage probability (purple) with $N_b = 40$.

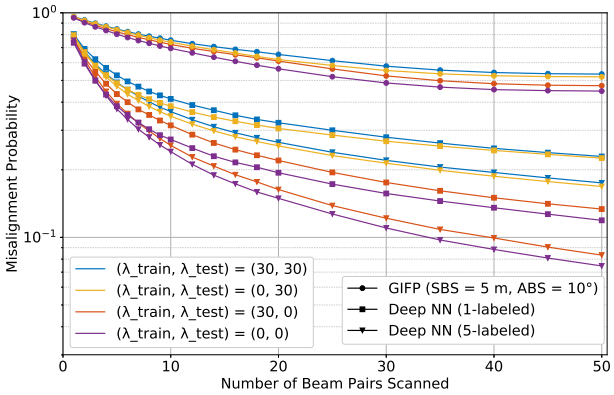

Fig. 7. Misalignment probability with mismatch in the number of mobile objects in train and test data.

of beam alignment dropped significantly with a mismatch in the number of mobile vehicles in training and test samples [3]. In order to evaluate the effects of this mismatch on our proposed solution and scenario, Fig.7 shows the misalignment probability of GIFP and deep NN methods when trained on an environment with mean number of mobile objects λ_{train} and evaluated in an environment with mean number of mobile objects λ_{test}. The results show that both the GIFP and Deep NN methods are fairly robust to this mismatch in our problem, contrary to the findings in [3]. We attribute this difference to larger degree of randomness in location and orientation in our setup, compared to the very structured distribution of mobile reflectors in vehicular applications.

V. Conclusions

Location information has valuable potential to reduce the overhead of initial access in indoor mmWave networks. In this paper, we proposed a beam alignment procedure by exploiting both position and orientation information of the receiver using machine learning. A deep neural network is trained to capture the most important beam directions for each receiver location in the training dataset and predicts the most powerful paths for unseen receiver positions and orientations.

We generalized the inverse fingerprinting beam alignment method to include orientation information as additional input in its procedure. We used this probabilistic method as baseline to be able compare our results with a well known, simple and data driven based algorithm. According to the numerical evaluations and comparisons, we observe that the proposed beam alignment approach outperforms the generalized inverse fingerprinting method. It is also shown that the proposed methods are robust to different configurations of mobile objects in the training and test data especially using multi-label classification by capturing more paths in each training sample. Overall, our results stand as proof of the superiority of deep neural networks as location-based beam selection method compared to other data-based approaches such as inverse fingerprinting.

References

[1] M. Giordani, M. Polese, M. Mezzavilla, S. Rangan, and M. Zorzi, "Towards 6G networks: Use cases and technologies," *arXiv*:1903.12216 [cs.NI], Mar. 2019. [Online]. Available: https://arxiv.org/abs/1903.12216.

[2] C. Liu and M. Li and S. V. Hanly and P. Whiting and I. B. Collings, "Millimeter-Wave small cells: Base station discovery, beam alignment, and system design challenges," *IEEE Wirel. Commun.*, vol. 25, no. 4, pp. 40–46, Aug. 2018.

[3] V. Va and J. Choi and T. Shimizu and G. Bansal and R. W. Heath, "Inverse multipath fingerprinting for millimeter wave V2I beam alignment," *IEEE Trans. Veh. Technol.*, vol. 67, pp. 4042–4058, May 2018.

[4] M. Giordani and M. Mezzavilla and M. Zorzi, "Initial access in 5G mmwave cellular networks," *IEEE Commun. Mag.*, vol. 54, no. 11, pp. 40–47, Nov. 2016.

[5] F. Maschietti and D. Gesbert and P. de Kerret and H. Wymeersch, "Robust location-aided beam alignment in millimeter wave massive MIMO," in *Proc. IEEE GLOBECOM*, Dec. 2017, pp. 1–6.

[6] V. Va and T. Shimizu and G. Bansal and R. W. Heath, "Position-aided millimeter wave V2I beam alignment: A learning-to-rank approach," in *Proc. IEEE 28th Annu. Int. Symp. Pers. Indoor Mobile Radio Commun.*, Oct. 2017, pp. 1–5.

[7] Y. Wang and A. Klautau and M. Ribero and A. C. K. Soong and R. W. Heath, "MmWave vehicular beam selection with situational awareness using machine learning," *IEEE Access*, vol. 7, pp. 87479–87493, Jun. 2019.

[8] N. González-Prelcic and R. Méndez-Rial and R. W. Heath, "Radar aided beam alignment in mmwave v2i communications supporting antenna diversity," in *Information Theory and Applications Workshop (ITA)*, Jan. 2016, pp. 1–7.

[9] M. Dias and A. Klautau and N. González-Prelcic and R. W. Heath, "Position and LIDAR-aided mmWave beam selection using deep learning," in *2019 IEEE 20th International Workshop on Signal Processing Advances in Wireless Communications(SPAWC)*, Jul. 2019, pp. 1–5.

[10] G. E. Garcia and G. Seco-Granados and E. Karipidis and H. Wymeersch, "Transmitter beam selection in millimeter-wave MIMO with in-band position-aiding," *IEEE Trans. Wireless Commun.*, vol. 17, no. 9, pp. 6082–6092, Sep. 2018.

[11] R. T. Rakesh, G. Das, and D. Sen, "An analytical model for millimeter wave outdoor directional non-line-of-sight channels," in *Proc. IEEE Int. Conf. Commun.*, May 2017, pp. 1–6.

[12] 3GPP, "Study on channel model for frequencies from 0.5 to 100 GHz," *3rd Gener. Partnership Project, Tech. Rep.* 38.901 V14.3.0, Dec. 2017.

[13] A. Ali and R. W. Heath, "Compressed beam-selection in millimeterwave systems with out-of-band partial support information," in *Proc. IEEE Int. Conf. Acoust., Speech Signal Process. (ICASSP)*, Mar. 2017, pp. 3499–3503.

[14] N. Srivastava, G. Hinton, A. Krizhevsky, I. Sutskever, and Ruslan Salakhutdinov, "Dropout: A simple way to prevent neural networks from overfitting," *J. Mach. Learn. Res.*, vol. 15, no. 1, pp. 1929–1958, Jan, 2014.